

Regioselectivity in the [2 + 2] cyclo-addition reaction of triplet carbonyl compounds to substituted alkenes (Paterno–Büchi reaction): A spin-polarized conceptual DFT approach

B PINTÉR,¹ F DE PROFT,² T VESZPRÉMI¹ and P GEERLINGS^{2,*}

¹Inorganic Chemistry Department, Budapest University of Technology and Economics (BUTE), Szent Gellért tér 4, H-1521, Budapest, Hungary

²Eenheid Algemene Chemie (ALGC), Vrije Universiteit Brussel (VUB), Faculteit, Wetenschappen, Pleinlaan 2, 1050 Brussels, Belgium
e-mail: pgeerling@vub.ac.be

Abstract. Regioselectivity of the photochemical [2 + 2] cyclo-addition of triplet carbonyl compounds with a series of ground state electron-rich and electron-poor alkenes, the Paterno–Büchi reaction, is studied. Activation barriers for the first step of the triplet reaction are computed in the case of the O-attack. Next, the observed regioselectivity is explained using a series of DFT-based reactivity indices. In the first step, we use the local softness and the local HSAB principle within a softness matching approach, and explain the relative activation barriers of the addition step. In the final step, the regioselectivity is assessed within the framework of spin-polarized conceptual density functional theory, considering response functions of the system's external potential v , number of electrons N and spin number N_s , being the difference between the number of a and b electrons in the spin-polarized system. Although the concept of local spin philicity, introduced recently within this theory, appears less suited to predict the regioselectivity in this reaction, the correct regioselectivity emerges from considering an interaction between the largest values of the generalized Fukui functions f_{ss} on both interacting molecules.

Keywords. Regioselectivity; cyclo-addition of triplet carbonyl compounds; spin-polarized conceptual DFT approach.

1. Introduction

The Paterno–Büchi reaction^{1–4} (figure 1), i.e. the formation of oxetanes via photochemical cyclo-addition of aldehydes and ketones to alkenes, is the most general method for the synthesis of four-membered oxygen heterocyclic rings (oxetanes) in a regio- and stereoselective manner. An impressive number of papers, both preparative^{5–8} and mechanistic,^{9–13} have been published in this field. Mechanistic studies have shown that the cyclo-addition generally proceeds through the attack of an (n, p^*) excited carbonyl compound on a ground-state olefin. For oxetane formation to occur, the excited state energy of the olefin must be higher than that of the ketone so that energy transfer does not dominate the reaction.^{14–17} The reaction occurs for both the first singlet and triplet^{1,3} (n, p^*) excited state of the carbonyl compounds.^{3,4} The reaction is known to proceed via 1,4-diradicals which were detected experimentally in transient spectroscopy studies.¹⁸ The

Paterno–Büchi cyclo-addition, proceeding through triplet manifold, exhibits good regio- and stereoselectivity and the most general adopted method to predict the major product is the most stable biradical rule, which was predicted first by Zimmerman.¹⁹ There are exceptions to this rule; special methods were suggested to predict the major product, for example attack on the less hindered side of the molecule, the relative stability of the adducts²⁰ or kinetic control.²¹

Rationalization of the model of cyclo-addition to unsymmetrical substituted olefins²⁰ has also led to postulating a nonconcerted mechanism (predominant isomer), and the results show that product ratios are not always simply predicted from the stability of the

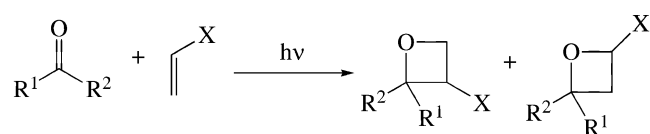


Figure 1. [2+2] Photo-cyclo-addition of a triplet carbonyl compound to a singlet ethylene.

*For correspondence

intermediate radicals. The results suggest that the additions occur via one excited quenchable state, most likely the (n, \mathbf{p}^*) triplet state of the carbonyl compounds. Other regio- and stereoselective Paterno–Büchi reactions involve the use of phenylglyoxylates as the olefin components²² and numerous electron-rich and electron-poor alkenes at the olefin side. The results clearly demonstrate that the electron density of the olefins affects the mechanism; the reaction for electron-rich alkenes is rapid, highly regio- and stereoselective, without competitive Norrish type II reactions. When less electron-rich alkenes are used, the Norrish type II reaction becomes competitive. One can predict the regioselectivity with the “biradical rule”, the instant of the intersystem crossing determines the stereoselectivity of the products.

In contrast to unsymmetrically substituted allenes, in the case of 9-methyl-1,2-butadiene, lower regioselectivity, but higher stereoselectivity was found.²³ In the reaction between styrene and benzaldehyde²⁴ there is a $\mathbf{p-p}$ overlap which has an impact on the distribution of products because there is *cis*-2,2-diphenyloxetane obtained from the irradiation. For silylated cinnamyl alcohol and benzaldehyde noncovalent tethering was reported (but not $\mathbf{p-p}$ overlap) since there is only one stereoisomer obtained and no side reactions. If tethering is involved, then phenyl groups must be held in opposite directions in the coordinated structure due to steric effects. Recently, a couple of studies reported the hydrogen-bond interaction in the excited singlet and triplet states,^{25,26} influencing the ratio of regio- and stereoisomers. Palmer *et al*⁹ performed a detailed MC-SCF/6-31G* study of the singlet and triplet Paterno–Büchi reaction using formaldehyde and ethylene as model systems, investigating both the formation of the oxetane via carbon–carbon and carbon–oxygen attacks. They found the C–O attack to be non-concerted, the first step of the reaction involving, in the case of the triplet pathway, the direct formation of the diradical intermediate. One of their other conclusions stated that the triplet diradicals generated in this reaction have similar energies and geometries to the singlets. Nguyen *et al*¹¹ used the Fukui functions, the local softness and the local hard and soft acids and bases principle for the regioselectivity of oxetane formation in the lowest $^3(n, \mathbf{p}^*)$ state of carbonyl compounds and their results are in good agreement with the experimental data. In their approach, they considered this reaction to be a concerted one-step cyclo-addition. In 2004, D’Auria *et al*²⁰ reported that an approach based on the frontier orbitals control is more efficient in explaining the photochemical

behavior for furan derivatives than the most stable biradical rule.

In this contribution, we carry out a high level theoretical study on the regioselectivity of the Paterno–Büchi photocyclo-addition of triplet acetone and acetophenone on a series of substituted alkenes, involving both electron-poor and electron-rich alkenes. Next to the localization of the transition structures of the biradical formation step of this reaction, the regioselectivity is assessed within the framework of both non-spin polarized and spin-polarized conceptual density functional theory.²⁷

2. Theory and computational details

Next to the well-established computational advantages, density functional theory (DFT) is the source for the introduction of a series of concepts and principles, readily used by chemists but often defined on an empirical basis. This aspect of DFT, in which chemical quantities are identified with response functions of the system’s energy with respect to either the number of electrons N , the external (i.e. due to the nuclei) potential $v(\mathbf{r})$ or both was termed “conceptual DFT” by R G Parr. The first-order derivative of the energy of the system with respect to the number of electrons is the chemical potential \mathbf{m} identified by Parr *et al*^{28,29} with the negative of the electronegativity \mathbf{c} :

$$\mathbf{m} = -\mathbf{c} = (\partial E / \partial N)_v \quad (1)$$

The chemical hardness \mathbf{h} of the system³⁰ was quantified by Parr and Pearson as:³¹

$$\mathbf{h} = \frac{1}{2} (\partial^2 E / \partial N^2)_v \quad (2)$$

which, in a finite difference approximation, can be written as:

$$\mathbf{h} \approx (IE - EA)/2, \quad (3)$$

where IE and EA are the vertical ionization energy and electron affinity of the systems respectively. The inverse of the global hardness is the global softness S :³²

$$S = 1/\mathbf{h} = (\partial N / \partial \mathbf{m})_v \approx 1/(IE - EA). \quad (4)$$

The local counterpart of this quantity, the local softness $s(\mathbf{r})$, is introduced as:^{32,33}

$$s(\mathbf{r}) \equiv \left(\frac{\partial \mathbf{r}(\mathbf{r})}{\partial \mathbf{m}} \right)_v = \left(\frac{\partial \mathbf{r}(\mathbf{r})}{\partial N} \right)_v \left(\frac{\partial N}{\partial \mathbf{m}} \right) = S f(\mathbf{r}), \quad (5)$$

where $f(\mathbf{r})$ is the Fukui function, a reactivity index introduced by Parr and Yang.³⁴ Due to the discontinuity of the electron density with respect to the number of electrons, three different Fukui functions can be introduced, representing the case of a nucleophilic attack (f^+), an electrophilic attack (f^-) or a neutral (radical) attack (f^0):

$$f^+ \equiv (\partial \mathbf{r}(\mathbf{r}) / \partial N)_v^+ \approx \mathbf{r}_{N+1}(\mathbf{r}) - \mathbf{r}_N(\mathbf{r}), \quad (6)$$

$$f^- \equiv (\partial \mathbf{r}(\mathbf{r}) / \partial N)_v^- \approx \mathbf{r}_N(\mathbf{r}) - \mathbf{r}_{N-1}(\mathbf{r}), \quad (7)$$

$$f^0 \equiv (f^+ + f^-) / 2 \approx 1/2(\mathbf{r}_{N+1}(\mathbf{r}) - \mathbf{r}_{N-1}(\mathbf{r})), \quad (8)$$

where $\mathbf{r}_{N+1}(\mathbf{r})$, $\mathbf{r}_N(\mathbf{r})$ and $\mathbf{r}_{N-1}(\mathbf{r})$ are the electron densities of the $N + 1$, N and $N - 1$ electron system respectively, all obtained at the geometry of the N -electron system, due to the fact that the derivative is taken at a constant external potential. These Fukui functions can be condensed to the nuclei by using an atomic charge partitioning scheme, $N_k(N + 1)$, $N_k(N)$ and $N_k(N - 1)$ representing the electron populations on atom k in the $N + 1$, N and $N - 1$ electron system.³⁵

$$f_k^+ \approx N_k(N + 1) - N_k(N), \quad (9)$$

$$f_k^- \approx N_k(N) - N_k(N - 1), \quad (10)$$

$$f_k^0 \approx \frac{1}{2}(N_k(N + 1) - N_k(N - 1)). \quad (11)$$

The condensed local softness is the product of the global softness S with f_k^i at a given site k :

$$s_k^i = S \cdot f_k^i \quad (12)$$

where i equals either +, - or 0 depending on whether the system undergoes a nucleophilic, electrophilic or radical attack. A theoretical justification of the HSAB-principle was provided by Chattaraj, Lee and Parr.³⁶ This principle has been applied many times in recent years, both at the local and the global level, for the rationalisation of regioselectivity and reactivity of many problems.³⁷

The above mentioned response functions can be used to describe changes from one ground state to another. The Hohenberg–Kohn theorems,³⁸ on which density functional theory is based, were also initially

developed for the ground states but could later on be generalized to time-dependent electron densities and external potentials.^{39,40} Applications of these DFT based reactivity indices to excited states have moreover been scarce.⁴¹

In the present application, one of the reaction partners, i.e. the carbonyl compound, is in its excited triplet state for which the electron densities of the \mathbf{a} and \mathbf{b} electrons are different, corresponding to a spin-polarized chemical system. We are thus working within the framework of spin-polarized DFT.⁴² Galván, Vela and Gázquez have introduced spin-polarized conceptual DFT, deriving expressions for, among others, the spin potential μ_s , the spin hardness \mathbf{h}_{ss} and the Fukui functions f_{ss} .^{43a} (For a detailed account of other reactivity indices introduced within this framework, see ref. 43).

The spin potential \mathbf{m}_s is introduced as the partial derivative of the energy with respect to the spin number, $N_s (=N_a - N_b)$, since it provides a measure for the tendency of the system to change its spin polarization:

$$\mathbf{m}_s = (\partial E / \partial N_s)_{N, v(\mathbf{r}), \mathbf{B}}, \quad (13)$$

where \mathbf{B} is the external magnetic field.

The second-order partial derivative of the energy with respect to N_s is the spin hardness \mathbf{h}_{SS} :

$$\mathbf{h}_{SS} = (\partial \mathbf{m}_s / \partial N_s)_{N, v(\mathbf{r}), \mathbf{B}} = (\partial^2 E / \partial N_s^2)_{N, v(\mathbf{r}), \mathbf{B}}. \quad (14)$$

The change of the spin density $\mathbf{r}_s(\mathbf{r})$ upon change in spin number N_s is governed by the Fukui function f_{SS} :

$$f_{SS} = (\partial \mathbf{r}_s(\mathbf{r}) / \partial N_s)_{N, v(\mathbf{r}), \mathbf{B}}. \quad (15)$$

The total energy of a system can be expanded in a Taylor series around the reference ground state and the energy difference between the ground and promoted state, at constant total number of electrons and external potential, can be written up to second order as:

$$\Delta E_{v,N} \approx \mathbf{m}_s^0 + \frac{1}{2} \mathbf{h}_{ss}^0 (\Delta N_s)^2. \quad (16)$$

In this expression, \mathbf{m}_s^0 must always be calculated in a given direction, substituting \mathbf{m}_s^0 by \mathbf{m}_s^\dagger when describing changes with increasing spin number, and by \mathbf{m}_s^\ddagger when the spin number is decreasing. The chemical potentials \mathbf{m}_s^\dagger and \mathbf{m}_s^\ddagger can be approximated as:

$$\mathbf{m}_s^+ \approx (\mathbf{e}_{\text{LUMO}}^a - \mathbf{e}_{\text{HOMO}}^b)/2 \quad (17)$$

and

$$\mathbf{m}_s^- \approx (\mathbf{e}_{\text{HOMO}}^a - \mathbf{e}_{\text{LUMO}}^b)/2, \quad (18)$$

where $\mathbf{e}_{\text{HOMO}}^a$, $\mathbf{e}_{\text{HOMO}}^b$, $\mathbf{e}_{\text{LUMO}}^a$ and $\mathbf{e}_{\text{LUMO}}^b$ are the orbital energies of the **a** and **b** HOMO and LUMO orbitals respectively. The spin hardness can be evaluated as:

$$\mathbf{h}_{SS}^0 \approx [\mathbf{m}_s^-(M') - \mathbf{m}_s^+(M)]/2, \quad (19)$$

where $\mathbf{m}_s^-(M')$ is the spin potential of the higher multiplicity (M'), towards a decrease in the spin number and $\mathbf{m}_s^+(M)$ the spin potential of the lower multiplicity (M) towards an increase in N_s . It measures the curvature of the E versus N_s curve in the given interval. Within this framework, Pérez *et al*⁴⁴ defined the concepts spin-philicity and spin-donicity. The spinphilicity index \mathbf{w}_s^+ of the system can be defined as:⁴⁴

$$\mathbf{w}_s^+ \equiv (\mathbf{m}_s^+)^2/2\mathbf{h}_{SS}. \quad (20)$$

In the direction of a decreasing spin number, the spin-donicity index is given as:

$$\mathbf{w}_s^- \equiv (\mathbf{m}_s^-)^2/2\mathbf{h}_{SS}. \quad (21)$$

Both indices are shown to be interesting quantities in the discussion of spin catalysis phenomena and can be invoked to explain singlet–triplet gaps.^{41f,41g} De Proft *et al*⁴⁵ introduced the concepts of local spin-philicity and donicity for use in regioselectivity studies. The spin-philicity can be calculated condensed on a atom k in the molecule, as:

$$\mathbf{w}_{s,k}^+ = [(\mathbf{m}_k^+)^2/2\mathbf{h}_{SS}]f_{s,s,k}^+, \quad (22)$$

where $f_{s,s}^+$ denotes the spin Fukui function in the direction of increasing spin number. Similarly we define the local spin-donicity, condensed on an atom k , as:

$$\mathbf{w}_{s,k}^- = [(\mathbf{m}_k^-)^2/2\mathbf{h}_{SS}]f_{s,s,k}^-, \quad (23)$$

$f_{s,s}^-$ being the Fukui function for decreasing spin number. Approximations for these spin Fukui functions can be computed using the approximations proposed by Galvan *et al*^{43a}:

$$f_{s,s}^+(\mathbf{r}) \approx \frac{1}{2}[|\mathbf{f}_{\text{LUMO},a}|^2 + |\mathbf{f}_{\text{HOMO},b}|^2], \quad (24)$$

$$f_{s,s}^-(\mathbf{r}) \approx \frac{1}{2}[|\mathbf{f}_{\text{HOMO},a}|^2 + |\mathbf{f}_{\text{LUMO},b}|^2], \quad (25)$$

where $\mathbf{f}_{\text{HOMO},a}$, $\mathbf{f}_{\text{HOMO},b}$, $\mathbf{f}_{\text{LUMO},a}$ and $\mathbf{f}_{\text{LUMO},b}$ are respectively the **a** and **b** HOMO and LUMO orbitals.

These concepts were successfully applied in study of the regioselectivity of the [2 + 2] cyclo-addition of triplet enones on substituted alkenes.⁴⁵ All calculations were performed at the (U)B3LYP level⁴⁶ using the Gaussian 03 program.⁴⁷ The different triplet carbonyl compounds and singlet alkenes studied are given in figure 2. All transition state geometries of the first addition step of the reaction on the triplet energy surface were optimized using the (U)B3LYP level of theory with the 6-31G(*d*) basis set. The geometries used to compute the DFT based reactivity indices were fully optimized with the 6-311+G** basis set⁴⁸ and were confirmed to be minima on the potential energy surface. Molecular properties and reactivity indices were obtained at the 6-311G** level; as can be seen, the diffuse function in the basis set used for the optimization of the reacting molecules was dropped when computing the properties because this was found to be more suitable in the case of the Fukui functions and local softnesses, where anionic metastability is frequently observed (for a detailed account, see ref. [27g]). Atomic populations were obtained using the natural population analysis (NPA),⁴⁹ in order to compute the condensed Fukui functions and local softnesses. The Fukui functions $f_{s,s}$ were computed

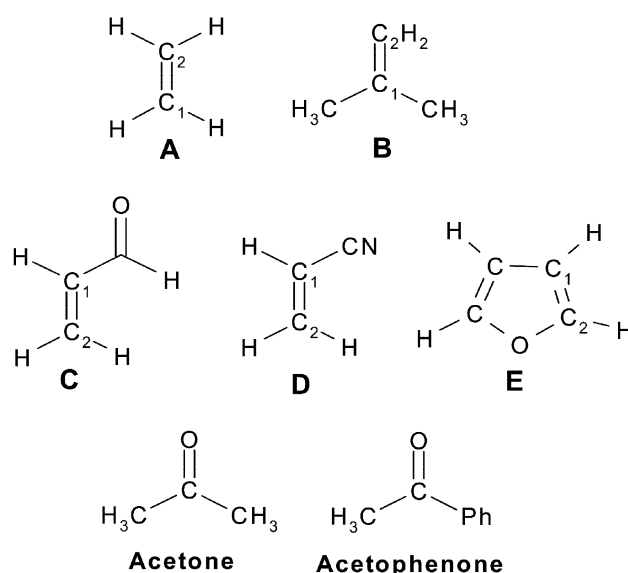


Figure 2. Different compounds investigated in this work: A = ethylene, B = isobutene, C = acrylonitrile, D = acrolein, E = furan.

using approximations (24) and (25); the condensed values of densities of **a** and **b** frontier molecular orbitals on the different atoms were obtained using the Hirshfeld partitioning scheme.⁵⁰ This partitioning scheme has also been found particularly useful to compute condensed values of DFT-based reactivity indices.⁵¹

3. Results and discussion

In the first part of this work, we have investigated the reaction mechanism in some more detail for our series of ketones and substituted ethylenes. The transition state (TS) structures for the first step (figure 3), i.e. the formation of the diradical structures, which are the intermediates of the reaction, were located. In this work, we have only investigated the triplet surface of the attack of the carbonyl oxygen to one of the carbon atoms of the substituted ethylenes. In figure 4, the two different orientations for the carbonyl oxygen attack are depicted: the face-to-face and the face-to-edge attack. In the face-to-face attack, an electron on the carbonyl oxygen and an electron on an olefin carbon are spin-coupled to form a CO bond while the carbonyl and alkene fragments are mutually parallel. When the carbonyl oxygen attacks the olefin in a perpendicular orientation, the face-to-edge attack, the terminal groups on the carbonyl are rotated by approximately 90 degrees. As is generally accepted that the face-to-edge

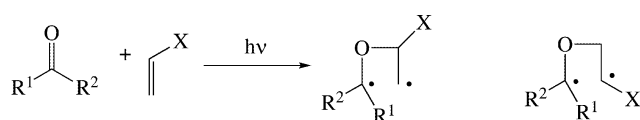


Figure 3. First step (C–O attack) of the [2 + 2] photo-cyclo-addition of a triplet carbonyl compound to a singlet ethylene.

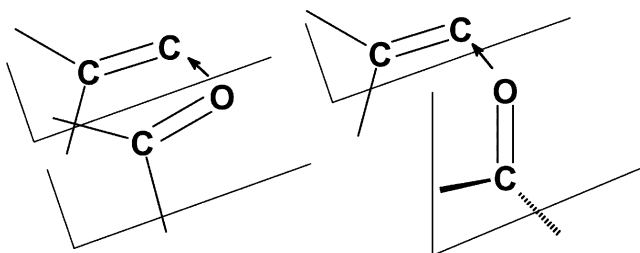


Figure 4. The two different orientations for the carbonyl oxygen attack: the face-to-face (left) and the face-to-edge (right) attack.

attack correlates electronically with an (*n*, *p*^{*}) excited-state carbonyl compound and a ground state olefin, our attention was mainly focussed on this orientation in the optimization of the different transition states. The different arrangements of the transition states for the C–O attack that were considered in this work are presented in figure 5.

It indeed turns out that the majority of the optimized transition states correspond to a face-to-edge arrangement. In the case of the transition states for the attack of acetone and acetophenone to the substituted carbon atom of the electron poor alkenes, one face-to-edge and one face-to-face (the dihedral angle is $\approx 10^\circ$) transition states are formed. During the face-to-edge attack on C₁ of propenal, in addition to the negative direction of curvature corresponding to forming the C–O bond, there is a force constant for the rotation of the ethylenic terminal methylene. Because of this, the transition structure could not be optimized accurately. The attack of the carbonyl oxygen to the C₁ of isobutene was found to occur via face-to-face orientation. As can be seen for the activation barriers listed in table 1, for all compounds, the lowest activation barrier is observed for the attack of the carbonyl oxygen on the least substituted carbon atom of the olefin, in agreement with experiment (for the case of furan) and Markovnikov's rule.

Table 1. Activation barriers (ΔE and ΔG) for the first step (addition of the carbonyl oxygen to the double bond of the alkenes) in the [2 + 2] photo-cyclo-addition of acetone and acetophenone to the substituted alkenes considered. All values were obtained at the B3LYP/6-311+G**//B3LYP/6-31G* level and are given in kcal/mol.

Alkene	Structure	Acetone		Acetophenone	
		ΔE	ΔG	ΔE	ΔG
Ethylene	A	5.4	17.2	6.1	18.7
Isobutene	B1	5.3	16.3	6.1	19.5
	B2	2.7	15.3	3.2	16.3
Acrolein	C1	4.9	16.4	8.5	21.0
	C2	4.0	15.9	4.4	17.4
	C2'	4.4	16.9	6.6	19.2
Acrylonitrile	D1	5.9	16.8	9.3	21.9
	D1'	5.6	17.0	6.6	19.1
	D2	3.5	16.0	3.5	16.3
	D2'	3.7	16.1	4.3	17.4
Furan	E1	8.5	21.3	7.9	21.5
	E1'	11.1	24.0	10.6	24.0
	E2	2.7	15.3	3.4	16.7
	E2'	4.4	17.0	3.0	16.4

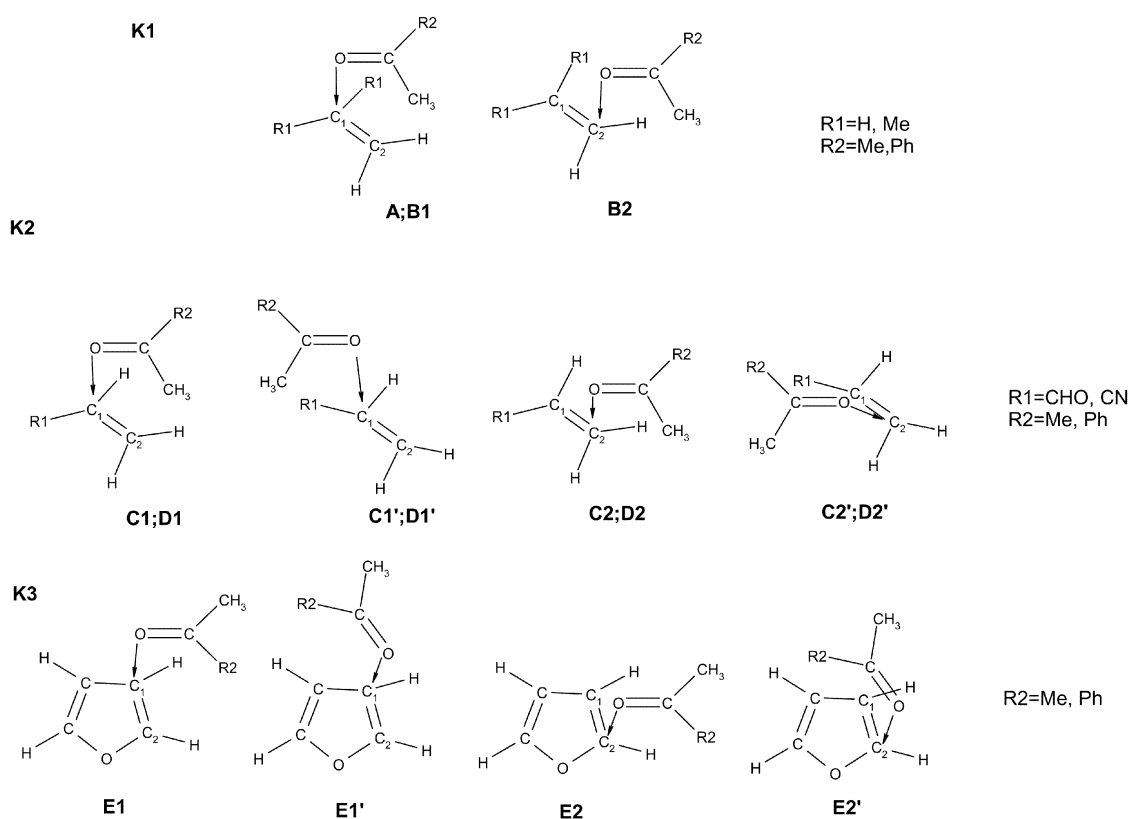


Figure 5. Structures of the different transition states obtained in this work.

Table 2. Vertical ionization energies I , electron affinities A , global softnesses S , condensed spin density N_s , Fukui functions f and local softnesses s for triplet acetone and acetophenone obtained at the B3LYP/6-311G**//B3LYP/6-311+G** level.

Molecule	I (eV)	A (eV)	S (a.u.)	Atom	N_s	f^- (a.u.)	f^+ (a.u.)	f^0 (a.u.)	s^- (a.u.)	s^+ (a.u.)	s^0 (a.u.)
Acetone	7.236	1.758	4.967	C	0.705	0.401	0.014	0.207	1.990	0.070	1.030
				O	1.056	0.204	0.562	0.383	1.014	2.791	1.902
Acetophenone	6.209	2.850	8.101	C	0.474	0.252	-0.068	0.092	2.043	-0.549	0.747
				O	1.041	0.103	0.541	0.322	0.835	4.379	2.607

Next, we assess the regioselectivity of the first addition step of the oxygen of the triplet carbonyl compounds to the alkenes using the well-known “non-spin-polarized” DFT based reactivity indices and the local hard and soft acids and bases principle.³⁷ In this approach, one is looking at the softness resemblance of the interacting sites, in this case by considering the smallest absolute value of the difference in local softness between the oxygen of either the triplet acetone or acetophenone on the one hand and one of the carbon atoms of the double bond (C_1 or C_2) in the alkenes on the other, i.e. considering:

$$\sum_0^1 = |s_0 - s_{C1}|, \quad (26)$$

$$\sum_0^2 = |s_0 - s_{C2}|, \quad (27)$$

This approach has been termed “softness-matching”.³⁷

Within this approach we can either use the s^+/s^- -softnesses, considering the interaction to be an interaction between an electrophile and a nucleophile, which was adopted in the work of Nguyen *et al.*¹¹ We could also perform the softness matching using

Table 3. Vertical ionization energies I , electron affinities A , global softnesses S , Fukui functions f and local softnesses s for the singlet alkenes obtained at the B3LYP/6-311G**//B3LYP/6-311+G** level.

Molecule	I (eV)	A (eV)	S (a.u.)	Atom	f^- (a.u.)	f^+ (a.u.)	f^0 (a.u.)	s^- (a.u.)	s^+ (a.u.)	s^0 (a.u.)
Ethylene	10.556	-2.761	2.043	C ₁ =C ₂	0.423	0.386	0.404	0.863	0.790	0.826
Isobutene	9.239	-2.639	2.291	C ₁	0.268	0.165	0.217	0.615	0.379	0.497
				C ₂	0.379	0.322	0.351	0.868	0.739	0.803
Acrylonitrile	10.727	-0.638	2.394	C ₁	0.205	0.205	0.205	0.492	0.490	0.491
				C ₂	0.321	0.347	0.334	0.768	0.831	0.800
Acrolein	9.903	-0.447	2.629	C ₁	-0.018	0.090	0.036	-0.047	0.238	0.095
				C ₂	0.194	0.305	0.249	0.510	0.801	0.655
Furan	8.892	-2.556	2.377	C ₁	0.120	0.095	0.107	0.285	0.225	0.255
				C ₂	0.265	0.247	0.256	0.631	0.587	0.609

Table 4. Transfer energies for one electron from the triplet carbonyl compound to the alkene ($I_{\text{carb}} - A_{\text{alkene}}$) and vice versa ($I_{\text{alkene}} - A_{\text{carb}}$), obtained at the B3LYP/6-311G**//6-311+G** level. All values are in eV.

Enone	Alkene	$I_{\text{carb}} - A_{\text{alkene}}$	$I_{\text{alkene}} - A_{\text{carb}}$
Acetone	Ethylene	10.00	8.80
	Isobutene	9.88	7.48
	Acrylonitrile	7.87	8.97
	Acrolein	7.68	8.15
	Furan	9.79	7.13
Acetophenone	Ethylene	8.97	7.71
	Isobutene	8.85	6.39
	Acrylonitrile	6.85	7.88
	Acrolein	6.66	7.05
	Furan	8.76	6.04

the local softness for a radical attack s^0 for both reagents, assuming the reaction to be a radical-radical interaction. In tables 2 and 3, the reactivity descriptors for the triplet carbonyl compounds and the singlet alkenes are listed. Using the vertical ionization energy (I) and electron affinity (A) one can approximate the energy needed to move an electron from the carbonyl compound to the alkene ($I_{\text{carb}} - A_{\text{alkene}}$) and the energy needed to move an electron from the alkene to the enone ($I_{\text{alkene}} - A_{\text{carb}}$). These transfer energies are listed in table 4. As can be seen, for the interaction of the triplet carbonyl compounds and the electron-rich alkenes, including ethylene, the transfer energy for an electron from the alkene to the excited carbonyl compound is lower than the reverse process, corresponding to an interaction of an electrophilic excited state species with the ground state alkene. In this case, one thus has to consider s^+ on the carbonyl compound and s^- on the alkenes. For the reaction with the electron-poor alkenes (i.e. acry-

lonitrile and acrolein), the transfer energy for an electron from the triplet carbonyl compounds to the alkenes is the lowest. It thus appears that these alkenes are now operating as electrophilic species, and one thus considers s^+ for these compounds in (26) and (27) together with s^- for the triplet carbonyl compounds.

The values of Σ_0^1 and Σ_0^2 obtained for the addition of the triplet carbonyl compounds to the alkenes, computed using (26) and (27), considering either an interaction between a nucleophile and an electrophile (s^+/s^-) or the interaction between two radicals (s^0/s^0) are listed in table 5. As can be seen, the smallest softness difference always occurs for the interaction of the oxygen of the triplet carbonyl compound with carbon atom 2 of the alkenes, in agreement with the computed activation barriers for this first addition step. From table 1, it can indeed be seen that the activation barrier for the addition of the oxygen atom on carbon 2 is always the lowest.

Finally, we investigate the regioselectivity in the different cases studied within the framework of spin-polarized conceptual DFT, as this reaction involves a singlet alkene and a triplet carbonyl compound. In the spin-polarized approach, the first step of this reaction can now be divided into two parts, both at constant external potential v , as schematically shown in figure 6. In the first step, a rearrangement of the spin density occurs in both reacting molecules. This amounts to a decrease of the spin number on the excited **a**, **b**-unsaturated carbonyl compound, resulting in stabilisation, and an increase of the spin number on the alkene, resulting in destabilization of the latter. The magnitude of the change of the spin density of the different sites in the interacting molecules upon a change of their total spin number N_s is governed by the generalized Fukui function given in (15); for

Table 5. The values of Σ_0^i for the addition of the triplet carbonyl compounds to the alkenes.

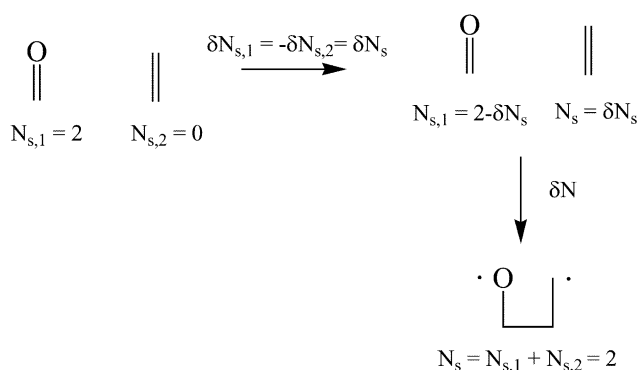
Values computed using (24), considering either an interaction between a nucleophile and an electrophile (s^+/s^-), or the interaction between two radicals (s^0/s^0). All values are in a.u.

Alkene		Acetone		Acetophenone	
		s^+/s^-	s^0/s^0	s^+/s^-	s^0/s^0
Ethylene	$\Sigma_0^1 = \Sigma_0^2$	1.927	1.076	3.516	1.781
Isobutene	Σ_0^1	2.176	1.405	3.764	2.110
	Σ_0^2	1.923	1.099	3.511	1.804
Acrylonitrile	Σ_0^1	0.525	1.412	0.345	2.116
	Σ_0^2	0.183	1.103	0.004	1.807
Acrolein	Σ_0^1	0.777	1.807	0.597	2.512
	Σ_0^2	0.214	1.247	0.034	1.952
Duran	Σ_0^1	2.506	1.648	4.095	2.352
	Σ_0^2	2.160	1.294	3.749	1.998

Table 6. Values of the density of the **a** HOMO, the **a** LUMO, the **b** HOMO and **b** LUMO orbitals, condensed to the O and C₂ atoms of the triplet carbonyl compounds, using the Hirshfeld partitioning scheme.

In the last column, the condensed generalized Fukui function f_{ss}^- , obtained using (24) and (25) is given. All values are in a.u.

Enone	Atom	$ f_{\text{HOMO},a} ^2$	$ f_{\text{LUMO},a} ^2$	$ f_{\text{HOMO},b} ^2$	$ f_{\text{LUMO},b} ^2$	f_{ss}^-
Acetone	C	0.519	0.045	0.149	0.091	0.305
	O	0.219	0.021	0.669	0.718	0.468
Acetophenone	C	0.313	0.007	0.005	0.085	0.199
	O	0.134	0.002	0.009	0.729	0.432

**Figure 6.** Spin-polarized description of the first step of the Paterno–Büchi reaction (constant external potential). In the first step, a spinpolarization of both reacting molecule occurs (change in N_s), followed by the charge transfer (change in the number of electrons N of both reacting species), forming the 1,4-biradical intermediate of the reaction.**Table 7.** Spin potentials of the singlet ground state $\bar{m}^\dagger(S_0)$, the triplet excited state $\bar{m}^\dagger(T_1)$, the spin hardnesses h_{SS}^0 and the spin philicities w_s^\dagger of the singlet alkenes. All values are in a.u.

Alkene	$\bar{m}^\dagger(T_1)$	$\bar{m}^\dagger(S_0)$	h_{SS}^0	w_s^\dagger
Ethylene	0.0257	0.1404	-0.0573	-0.1718
Isobutene	0.0283	0.1327	-0.0522	-0.1687
Acrylonitrile	0.0221	0.1162	-0.0470	-0.1436
Acrolein	0.0204	0.0952	-0.0374	-0.1212
Furan	0.0346	0.1169	-0.0412	-0.1660

the triplet carbonyl compound, this Fukui function has to be computed in the direction of decreasing N_s , whereas for the singlet alkenes, the direction of increasing N_s has to be considered. These condensed generalised Fukui functions, computed using the approximations given in (24) and (25), are given in table

Table 8. Values of the density of the **a** HOMO (= **b** HOMO) and the **a** LUMO (= **b** LUMO) orbitals, condensed to the C₁ and C₂ atoms of the singlet alkenes considered in this work, using the Hirshfeld partitioning scheme. In the last two columns, the condensed generalized Fukui function f_{ss}^+ , obtained using (36) is given, together with the local spin-philicities w_s^+ . All values are in a.u.

Alkene	Atom	$ f_{\text{HOMO},a} ^2$	$ f_{\text{LUMO},a} ^2$	f_{ss}^+	w_s^+
Ethylene	C ₁	0.439	0.398	0.418	-0.072
	C ₂	0.439	0.398	0.418	-0.072
Isobutene	C ₁	0.312	0.315	0.314	-0.053
	C ₂	0.433	0.347	0.390	-0.066
Acrylonitrile	C ₁	0.245	0.245	0.245	-0.035
	C ₂	0.316	0.363	0.340	-0.049
Acrolein	C ₁	0.087	0.161	0.124	-0.015
	C ₂	0.015	0.292	0.154	-0.019
Furan	C ₁	0.149	0.124	0.136	-0.023
	C ₂	0.296	0.243	0.269	-0.045

6 for the triplet carbonyl compounds (f_{ss}^-) and in table 8 for the singlet alkenes (f_{ss}^+). As can be seen, f_{ss}^+ is always the largest on the carbonyl oxygen atom of the triplet carbonyl compounds, in agreement with the NPA spin density values N_s given in table 2 for these compounds. In the case of the alkenes, f_{ss}^+ is always higher on the C₂ atom of the double bond. It thus appears that the correct regioselectivity can be predicted by presuming a spin coupling (first step in figure 6) of these two sites that exhibit the largest values of the generalized Fukui function. This finding seems to be reminiscent of some kind of hard and soft acids and bases principle within the context of spin-polarized DFT.

Table 7 lists the spin potentials, spin hardnesses and the global spin-philicities of the singlet alkenes studied in this work. As can be seen, all the spin-philicities are negative, in agreement with the fact that the energy change when going from the singlet state, the ground state, to the first excited triplet state (i.e. a change with $\Delta N_s = 2$) is positive. In previous work, this quantity has been proven to correlate with the singlet-triplet gaps of a series of singlet ground state carbenes, silylenes, germylenes and stannylenes. Recently, this correlation was confirmed by Olah *et al.*¹⁹ for a series of nitrenes and phosphinidenes. Table 8 lists the local spin-philicities of the different alkenes studied in this work. As can be seen, the most negative spin-philicities occur on C₂, in agreement with the fact that the condensed value of f_{ss}^+ is always the largest on this atom. The local contribution of this atom in the energy rise due to

the increase of the spin number can thus considered to be larger than the contribution of C₁. In this case however, this does not seem to be the decisive factor in prediction of the regioselectivity.

4. Conclusions

In this contribution, we have presented a study of the regioselectivity of the photochemical [2 + 2] cyclo-addition of carbonyl compounds with ground state alkenes, the Paterno-Büchi reaction, using DFT-based reactivity descriptors.

In a first part, we have located the different transition states for the first radical coupling step on the triplet surface for the reaction of triplet acetone and acetophenone with a series of electron-rich and electron-poor alkenes, focussing our attention exclusively on the O-attack. Next, we have investigated the regioselectivity using the local softness within the framework of the local hard and soft acids and bases principle. Within this approach, the interaction was investigated as either the interaction between a nucleophile and an electrophile or the interaction of two radicalar species on the other hand. Both approaches systematically yield a regioselectivity that is completely in agreement with the computed activation barriers.

Finally, the regioselectivity of this reaction was investigated using chemical concepts introduced within the framework of spin-polarized conceptual DFT. In this case, the local spin-philicity does not appear the

determining factor for the observed regioselectivity. The correct regioselectivity emerges from considering an interaction between the sites that undergo the largest change in spin number when the total spin number of the molecule is changing.

Acknowledgements

FDP and PG wish to thank the VUB and the Fund for Scientific Research Flanders-Belgium (FWO) for continuous support. BP and TV thank an OTKA grant for financial support.

References

1. Paterno E and Chieffi G 1909 *Gazz. Chim. Ital.* **39** 341
2. Büchi G, Inman C G and Lipinsky E S 1954 *J. Am. Chem. Soc.* **76** 4327
3. Turro N J 1978 *Modern molecular photochemistry* (Menlo Park, CA: Benjamin/Cummings)
4. March J and Smith M B 2001 *March's advanced organic chemistry* (New York: Wiley)
5. Turro N J, Wriede P A, Dalton J C, Arnold D and Glick A 1968 *J. Am. Chem. Soc.* **90** 6863
6. Turro N J and Wriede P A 1968 *J. Am. Chem. Soc.* **90** 6863
7. Barltrop J A and Carless H A J 1972 *J. Am. Chem. Soc.* **94** 8761
8. Dowd P, Gold A and Sachdev K 1970 *J. Am. Chem. Soc.* **92** 5725
9. Palmer I J, Ragazos I N, Bernardi F, Olivucci M and Robb M A 1994 *J. Am. Chem. Soc.* **116** 2121
10. Kutateladze A G 2001 *J. Am. Chem. Soc.* **123** 9279
11. Sengupta D, Chandra A K and Nguyen M T 1997 *J. Org. Chem.* **62** 6404
12. Yang N C and Eisenhardt W 1971 *J. Am. Chem. Soc.* **93** 1279
13. Muller F and Mattay J 1993 *Chem. Rev.* **93** 99
14. Dowd P, Gold A and Sachdev K 1970 *J. Am. Chem. Soc.* **92** 5725
15. Arnold D R, Hinman R L and Glick A H 1964 *Tetrahedron Lett.* 1425
16. Arnold D R 1968 *Adv. Photochem.* **6** 301
17. Farid S, Hartman S E and DeBoer C D 1975 *J. Am. Chem. Soc.* **97** 808
18. Freilich S C and Peters K S 1985 *J. Am. Chem. Soc.* **107** 3819
19. Zimmerman H 1966 *Science* **153** 837
20. D'Auria M, Emanuele L and Racioppi R 2004 *J. Photochem. Photobiol.* **A163** 103
21. Ciufolini M C, Rivera-Fortin M A, Zuzukin V and Whitmire K H 1994 *J. Am. Chem. Soc.* **98** 1994
22. Hu S and Neckers D C 1997 *J. Org. Chem.* **62** 564
23. Howell A R, Fan R and Truong A 1996 *Tetrahedron Lett.* **37** 8651
24. Fleming S A and Gao J J 1997 *Tetrahedron Lett.* **38** 5407
25. Griesbeck A G and Bondock S 2001 *J. Am. Chem. Soc.* **123** 6191
26. Adam W, Peters K, Peters E M and Stegmann V R 2000 *J. Am. Chem. Soc.* **122** 2958
27. (a) Parr R G and Yang W 1989 *Density functional theory of atoms and molecules* (New York: Oxford University Press); (b) Parr R G and Yang W 1995 *Annu. Rev. Phys. Chem.* **46** 701; (c) Kohn W, Becke A D and Parr R G 1996 *J. Phys. Chem.* **100** 12974; (d) Chermette H 1999 *J. Comput. Chem.* **20** 129; (e) Geerlings P, De Proft F and Langenaeker W 1999 *Adv. Quant. Chem.* **33** 303; (f) Geerlings P and De Proft F 2002 *Int. J. Mol. Sci.* **3** 276; (g) Geerlings P, De Proft F and Langenaeker W 2003 *Chem. Rev.* **103** 1793
28. Parr R G, Donnelly R A, Levy M and Palke W E 1978 *J. Chem. Phys.* **68** 3801
29. For a detailed account on the different electronegativity scales introduced see e.g. Mullay J 1987 in *Electronegativity: Structure and bonding* (eds) K D Sen and C K Jørgenson (Berlin, Heidelberg: Springer-Verlag) vol 66, p. 1
30. (a) Pearson R G 1963 *J. Am. Chem. Soc.* **85** 3533; (b) Pearson R G 1997 *Chemical hardness* (New York: John Wiley & Sons)
31. Parr R G and Pearson R G 1983 *J. Am. Chem. Soc.* **105** 7512
32. Yang W and Parr R G 1985 *Proc. Natl. Acad. Sci. USA* **82** 6723
33. Lee C, Yang W and Parr R G 1988 *J. Mol. Struct. (Theochem.)* **163** 305
34. Parr R G and Yang W 1984 *J. Am. Chem. Soc.* **106** 4049
35. Yang W and Mortier W J 1986 *J. Am. Chem. Soc.* **106** 5708
36. Chattaraj P K, Lee H and Parr R G 1991 *J. Am. Chem. Soc.* **113** 1855
37. (a) Gázquez J L 1993 in *Chemical hardness: Structure and bonding* (ed.) K D Sen vol. 80, p. 27; (b) Méndez F and Gázquez J L 1994 *J. Am. Chem. Soc.* **116** 9298; (c) Gázquez J L and Méndez F 1994 *J. Phys. Chem.* **98** 4591; (d) Méndez F and Gázquez J L 1994 *Proc. Indian Acad. Sci.* **106** 183; (e) Damoun S, Van de Woude G, Méndez F and Geerlings P 1997 *J. Phys. Chem.* **A101** 886; (f) Geerlings P and De Proft F 2000 *Int. J. Quantum Chem.* **80** 227
38. Hohenberg P and Kohn W 1964 *Phys. Rev.* **136** B864
39. Runge E and Gross E K U 1984 *Phys. Rev. Lett.* **52** 997
40. Kohl H and Dreizler R M 1986 *Phys. Rev. Lett.* **56** 737
41. (a) Chattaraj P K and Poddar J 1998 *J. Phys. Chem.* **A102** 9944; (b) Chattaraj P K and Poddar J 1999 *J. Phys. Chem.* **A103** 1274; (c) Chattaraj P K and Poddar J 1999 *J. Phys. Chem.* **A103** 8691; (d) Sengupta D, Chandra A K and Nguyen M T 1997 *J. Org. Chem.* **62** 6404; (e) Mendez F and Garcia-Gariday M A *J. Org. Chem.* **64** 7061; (f) Oláh J, De Proft F, Veszprémi T and Geerlings P 2004 *J. Phys. Chem.* **A108** 490; (g) Oláh J, Veszprémi T and Nguyen M T 2005 *Chem. Phys. Lett.* **401** 337
42. (a) Von Bart U and Hedin L 1972 *J. Phys.* **C5** 1629; (b) Rajagopal A K and Callaway J 1973 *Phys. Rev.*

- B7** 1912; (c) Gunnarson O and Lundqvist B I 1976 *Phys. Rev.* **B13** 4274
43. (a) Galván M, Vela A and Gázquez J L 1988 *J. Phys. Chem.* **92** 6470; (b) Galván M and Vargas R 1992 *J. Phys. Chem.* **96** 1625; (c) Vargas R and Galván M 1996 *J. Phys. Chem.* **100** 14651; (d) Vargas R, Galván M and Vela A 1998 *J. Phys. Chem.* **A102** 3134; (e) Vargas R, Cedillo A, Garza J and Galván M 2002 In *Reviews of modern quantum chemistry: A celebration to the contributions of R G Parr* (ed.) K D Sen (Singapore, World Scientific) p. 936
44. Pérez P, Andrés J, Safont V S, Tapia O and Contreras R 2002 *J. Phys. Chem.* **A106** 5353
45. De Proft F, Fias S, Van Alsenoy C and Geerlings P 2005 *J. Phys. Chem.* **A108** 6335
46. (a) Becke A D 1993 *J. Chem. Phys.* **98** 5648; (b) Lee C, Yang W and Parr R G 1988 *Phys. Rev.* **B37** 785; (c) Stevens P J, Delvin F J, Chablaoski C F and Frisch M J 1994 *J. Phys. Chem.* **98** 11623
47. Frisch M J *et al* 2004 Gaussian 03 Revision B03, Gaussian Inc., Wallingford, CT
48. For a detailed account on these types of basis sets see e.g. W J Hehre, L Radom, P v R Schleyer and J A Pople 1986 *Ab initio molecular orbital theory* (New York: Wiley)
49. (a) Reed A E, Weinstock R B and Weinhold F 1985 *J. Chem. Phys.* **83** 735; (b) Reed A E and Weinhold F 1985 *J. Chem. Phys.* **83** 1736; (c) Reed A E, Curtiss L A and Weinhold F 1988 *Chem. Rev.* **88** 899
50. Hirshfeld F L 1977 *Theor. Chim. Acta* **44** 129
51. (a) De Proft F, Van Alsenoy C, Peeters A, Langenaeker W and Geerlings P 2002 *J. Comput. Chem.* **23** 1198; (b) De Proft F, Vivas-Reyes R, Peeters A, Van Alsenoy C and Geerlings P 2003 *J. Comput. Chem.* **24** 463